Stabilizing a Pulsed Field Emission from an Array of Carbon Nanotubes

Roy Mahapatra, D., Anand, S.V., Sinha, N., and Melnik, R.V.N.

Carbon Nanotubes, Graphene, and Associated Devices II.
Proceedings of SPIE, Optics+Photonics, Vol. 7399,
Eds. M. Razeghi, D. Pribat, Y.-H. Lee, San Diego, California, USA,
ISBN: 9780819476890, pp. 73990M--73990-10 (10 pages), 2009.

Stabilizing a Pulsed Field Emission from an Array of Carbon Nanotubes

D. Roy Mahapatra[a], S. Anand[a], N. Sinha[b] and R.V.N. Melnik[c]

[a]Department of Aerospace Engineering, Indian Institute of Science, Bangalore 560012, India
[b]Department of Mechanical Engineering, Massachusetts Institute of Technology, Cambridge, MA 02139, USA
[c]M^{2}NeT Lab, Wilfrid Laurier University, Waterloo, ON N2L 3C5, Canada

ABSTRACT

In this paper, we propose a new design configuration for a carbon nanotube (CNT) array based pulsed field emission device to stabilize the field emission current. In the new design, we consider a pointed height distribution of the carbon nanotube array under a diode configuration with two side gates maintained at a negative potential to obtain a highly intense beam of electrons localized at the center of the array. The randomly oriented CNTs are assumed to be grown on a metallic substrate in the form of a thin film. A model of field emission from an array of CNTs under diode configuration was proposed and validated by experiments. Despite high output, the current in such a thin film device often decays drastically. The present paper is focused on understanding this problem. The random orientation of the CNTs and the electromechanical interaction are modeled to explain the self-assembly. The degraded state of the CNTs and the electromechanical force are employed to update the orientation of the CNTs. Pulsed field emission current at the device scale is finally obtained by using the Fowler-Nordheim equation by considering a dynamic electric field across the cathode and the anode and integration of current densities over the computational cell surfaces on the anode side. Furthermore we compare the subsequent performance of the pointed array with the conventionally used random and uniform arrays and show that the proposed design outperforms the conventional designs by several orders of magnitude. Based on the developed model, numerical simulations aimed at understanding the effects of various geometric parameters and their statistical features on the device current history are reported.

Keywords: Carbon nanotube, array, field emission, pulse, electron, phonon, x-ray, thin film

1. INTRODUCTION

Field emission from Carbon Nanotubes (CNTs) was first reported in 1995 by three research groups.[1–3] With significant research attention, CNTs are currently ranked among the best field emitters. CNTs grown on substrates are used as electron sources in field emission applications. Several studies have reported the use of CNTs in field emission devices (e.g., field emission displays, x-ray tube sources, electron microscopes, cathode-ray lamps, etc.)[4–6] Also, in recent years, conventional cold-cathodes have been realized in micro-fabricated arrays for medical x-ray imaging.[7] Field emission performance of a single isolated CNT is found to be remarkable. However, the situation becomes complex when an array of CNTs is used.[8] Use of arrays of CNTs is practical and economical since they can be grown easily on cathode substrates. In addition, their collective dynamics can be utilized in a statistical sense such that the average emission intensity is high enough, and at the same time, the collective dynamics lead to longer emission life. Details of modeling and simulations can be found in refs.[9–11] Field emission from CNTs is difficult to characterize using simple formula or data fitting, which is due to several physical phenomena involved: (1) electron-phonon interaction; (2) electromechanical force field leading to deformation of CNTs; and (3) ballistic transport induced thermal spikes, coupled with high dynamic

Further author information: (Send correspondence to R.V.N. Melnik)
D. Roy Mahapatra: E-mail: droymahapatra@aero.iisc.ernet.in, Telephone: 91 80 2293 2419
S. Anand: E-mail: sandeepva86@gmail.com
N. Sinha: E-mail: nsinha@mit.edu, Telephone: 1 617 715 5238
R.V.N. Melnik: E-mail: rmelnik@wlu.ca, Telephone: 1 519 884 0710 ext. 3662

Carbon Nanotubes, Graphene, and Associated Devices II, edited by Manijeh Razeghi, Didier Pribat, Young-Hee Lee,
Proc. of SPIE Vol. 7399, 73990M · © 2009 SPIE · CCC code: 0277-786X/09/$18 · doi: 10.1117/12.826166

stress, leading to degradation of emission performance. Detailed physics-based models of CNTs incorporating the first two aspects above have already been developed by the authors.[12,13] For a matrix of CNTs, an analytical estimate of field enhancement factor including the effect of Coulomb field, image potential and anode-cathode distance was reported by Wang *et al.*[14] Effects of vertical alignment of CNTs and substrates on the field emission current-voltage characteristics were studied experimentally by Chen *et al.*[15] Effect of spacing and diameter of CNTs in the arrays have been studied in ref.[16] Although advances in patterning of CNTs for field emission application have been made in recent time (see e.g., ref.[17]), design optimization issues aimed at better field emission devices to reduce the extent of electromechanical fatigues and to improve spatio-temporal localization of emitted electrons still remain open areas of research. With due success in designing such devices, various applications such as in-situ biomedical x-rays probes and thin film pixel based imaging technology, are of great significance.

In this paper, we report the collective field emission performance of a point shaped array of CNTs grown on a metallic surface as compared to arrays with other types of pattern. The results show a stabilized emission with higher magnitude of current density. Subsequently, the deformation of the CNTs indicate improved dynamic orientations of the tips which is also important for longer fatigue life. We analyze this new design concept in the light of various sources of electrodynamic force fields during electron emission from the CNT tips and their non-local interaction in the array.

2. MODEL FORMULATION

We first discuss the basic modeling framework in this section and then formulate the model of electrodynamic force field by considering individual CNTs in the array as reduced one-dimension elements for transport of electron.

Let N_T be the total number of carbon atoms (in CNTs and in cluster form) in a representative volume element ($V_{\text{cell}} = \Delta A d$), where ΔA is the cell surface interfacing the anode and d is distance between the inner surfaces of cathode substrate and the anode. Let N be the number of CNTs in the cell, and N_{CNT} be the total number of carbon atoms present in the CNTs. We assume that during field emission some CNTs are decomposed and form clusters. Such degradation and fragmentation of CNTs can be treated as the reverse process of CVD or a similar growth process used for producing the CNTs on a substrate. Hence,

$$N_T = N N_{CNT} + N_{\text{cluster}} \,, \tag{1}$$

where N_{cluster} is the total number of carbon atoms in the clusters in a cell at time t and is given by

$$N_{\text{cluster}} = V_{\text{cell}} \int_0^t dn_1(t) \,, \tag{2}$$

where n_1 is the concentration of carbon clusters in the cell. By combining Eqs. (1) and (2), one has

$$N = \frac{1}{N_{CNT}} \left[N_T - V_{\text{cell}} \int_0^t dn_1(t) \right] . \tag{3}$$

The number of carbon atoms in a CNT is proportional to its length. Let the length of a CNT be a function of time, denoted as $L(t)$. Therefore, one can write

$$N_{CNT} = N_{\text{ring}} L(t) \,, \tag{4}$$

where N_{ring} is the number of carbon atoms per unit length of a CNT and can be determined from the geometry of the hexagonal arrangement of carbon atoms in the CNT. By combining Eqs. (3) and (4), one can write

$$N = \frac{1}{N_{\text{ring}} L(t)} \left[N_T - V_{\text{cell}} \int_0^t dn_1(t) \right] . \tag{5}$$

In order to determine $n_1(t)$ phenomenologically, we employ a nucleation coupled model developed by us previously [12]. Based on the model, the rate of degradation of CNTs (v_{burn}) is defined as

$$v_{\text{burn}} = V_{\text{cell}} \frac{dn_1(t)}{dt} \left[\frac{s(s-a_1)(s-a_2)(s-a_3)}{n^2a_1^2 + m^2a_2^2 + nm(a_1^2 + a_2^2 - a_3^2)} \right]^{1/2}, \tag{6}$$

where a_1, a_2, a_3 are lattice constants, $s = \frac{1}{2}(a_1 + a_2 + a_3)$, n and m are integers ($n \geq |m| \geq 0$). The pair (n, m) defines the chirality of the CNT. Therefore, at a given time, the length of a CNT can be expressed as $h(t) = h_0 - v_{\text{burn}}t$, where h_0 is the initial average height of the CNTs and d is the distance between the cathode substrate and the anode. In the time-dependent simulation of collective emission from an array of CNTs, we update the height of the CNTs using the burning rate v_{burn}.

2.1 Electron gas flow

We express the surface electron density ($\tilde{n}$) in a CNT (assuming it as a continuum tube) as the sum of a steady (unstrained) part ($\tilde{n}_0$) and a dynamically strained part ($\tilde{n}_0$). Therefore, $\tilde{n} = \tilde{n}_0 + \tilde{n}_1$, where the steady part $\tilde{n}_0$ is the surface electron density corresponding to the Fermi level energy in the unstrained CNT and it can be approximated as[18] $\tilde{n}_0 = kT/(\pi b^2 \Delta)$, where k is Boltzmann's constant, T is the absolute temperature, b is the interatomic distance and Δ is the overlap integral ($\approx 2eV$ for carbon). The fluctuating part $\tilde{n}_1$ is inhomogeneous along the length of the CNTs. Actually, $\tilde{n}_1$ should be coupled nonlinearly with the deformation and the electromagnetic field.[19] However, in a simplified form, $\tilde{n}_1$ is primarily governed by one of the quantum-hydrodynamic equations. The deformation of CNTs during field emission is a combined effect of various electromechanical forces in a slow time scale and the fluctuation of the CNT sheet due to electron-phonon interaction in a fast time scale. Therefore, the total displacement u_{total} can be expressed as

$$u_{\text{total}} = u^{(1)} + u^{(2)}, \tag{7}$$

where $u^{(1)}$ and $u^{(2)}$ are the displacements due to electromechanical forces and fluctuation of CNT sheets due to electron-phonon interaction, respectively. The elements of displacement vector in the coordinate system (x', y', z') with z' being the tangent to the curved tube axis, can be written as

$$u^{(1)} = \{u^{(1)}_{x'}\ u^{(1)}_{z'}\}^T, \quad u^{(2)} = \{u^{(2)}_{x'}\ u^{(2)}_{z'}\}^T, \tag{8}$$

where $u_{x'}$ is the lateral displacement and $u_{z'}$ is the longitudinal displacement at a length-wise location of CNTs, where the CNT cross-sections are reduced to a point, thus by neglecting the radial breathing modes. Furthermore, for simplification in the analysis, we consider only one component of lateral motion and remove the y' dependence of the motion in the slow time scale. In the array, each CNT is treated as a one-dimensional elastic member discretized by fictitious segments and nodes with equivalent electronic charges lumped on the nodes. The electrodynamic force field is computed as discussed in ref.[20]

In the fast time scale, the displacement field $u^{(2)}$ is coupled with the density of state via the changes in the atomic coordinates due to electrodynamic force. The electrodynamic force field comprises of Coulomb force due to pair-wise interaction of CNTs in the array and the electrodynamic force due to conduction electrons within a CNT. The density of state is further influenced by the electromagnetic field and self-interaction potentials. Such a dynamic interaction between the electrons and the electromagnetic field can be expressed as[21]

$$\frac{\partial^2 \tilde{n}_1}{\partial t^2} - \frac{e\tilde{n}_0}{m_e}\frac{\partial E_{z'}}{\partial z'} - \alpha_2 \frac{\partial^2 \tilde{n}_1}{\partial z'^2} + \beta_2 \frac{\partial^4 \tilde{n}_1}{\partial z'^4} + \frac{\beta_2}{r^2}\frac{\partial^2}{\partial z'^2}\left(\frac{\partial^2 \tilde{n_1}}{\partial \theta_0^2}\right) + \frac{n_0}{m_e}\frac{\partial f_{lz'}}{\partial z'} - \frac{e\tilde{n}_0}{m_e}\frac{1}{r}\frac{\partial E_{\theta_0}}{\partial \theta_0}$$

$$-\frac{\alpha_2}{r^2}\frac{\partial^2 \tilde{n}_1}{\partial \theta_0^2} + \frac{\beta_2}{r^4}\frac{\partial^4 \tilde{n}_1}{\partial \theta_0^4} + \frac{\beta_2}{r^2}\frac{\partial^2}{\partial \theta_0^2}\left(\frac{\partial^2 \tilde{n}_1}{\partial z'^2}\right) + \frac{n_0}{m_e}\frac{1}{r}\frac{\partial f_{l\theta_0}}{\partial \theta_0} - \frac{en_0}{m_e}\frac{\partial E_r}{\partial r} + \frac{n_0}{m_e}\frac{\partial f_{lr}}{\partial r} + \frac{n_0}{m_e}\frac{\partial f_{pr}}{\partial r} = 0 \tag{9}$$

where (r, θ_0, z') defines the cylindrical coordinate system for a CNT with $r = R$ as the CNT radius, m_e is the effective mass of electron, α_2 is the speed of propagation of density disturbances, β_2 is the single electron excitation in the electron gas, f_l is the Lorentz force, f_p is the ponderomotive force, and $E_{z'}$, E_{θ_0} and E_r are the

axial, circumferential and out-of-plane components of the electric field, respectively. The electric field satisfies the Maxwell's equation for the effective medium:

$$\nabla^2 E - \mu\sigma\frac{\partial E}{\partial t} - \mu\epsilon\frac{\partial^2 E}{\partial t^2} = \mu\frac{\partial J}{\partial t} \ , \tag{10}$$

where μ, σ, ϵ, and J are the magnetic permeability, electric conductivity, electric permittivity, and electric current density in a CNT as an effective medium, respectively. The current density in the CNT sheet can be approximated as

$$J \approx e\tilde{n}(v_0 + \frac{\partial u^{(2)}_{z'}}{\partial t} + c_p\frac{\partial u^{(2)}_{z'}}{\partial z'}) \ , \tag{11}$$

where v_0 is the velocity of conduction electrons in the unstrained CNT, c_p is the phase speed of sound propagation along z' direction.

In the absence of electronic transport within and field emission from the tip of a CNT, the background electric field is simply $E_0 = -V_0/d$, where $V_0 = V_d - V_s$ is the applied bias voltage, V_s is the constant source potential on the substrate side, V_d is the drain potential on the anode side and d, as before, is the clearance between the electrodes. The total electrostatic energy consists of a linear drop due to the uniform background electric field and the potential energy due to the charges on the CNTs. Therefore, the total electrostatic energy can be expressed as

$$\mathcal{V}(x,z) = -eV_s - e(V_d - V_s)\frac{z}{d} + \sum_j G(i,j)(\hat{n}_j - n) \ , \tag{12}$$

where e is the positive electronic charge, $G(i,j)$ is the Green's function[22] with i indicating the ring position and $\hat{n}_j$ describing the electron density at node position j on the ring. In the present case, while computing the Green's function, we also consider the nodal charges of the neighboring CNTs. This essentially introduces non-local contributions due to the array of CNTs. We compute the total electric field $\mathbf{E} = -\nabla\mathcal{V}/e$, which is expressed as

$$E_z = -\frac{1}{e}\frac{d\mathcal{V}(z)}{dz} \ . \tag{13}$$

The current density (J) due to field emission is obtained by using the Fowler-Nordheim equation[23]

$$J = \frac{BE_z^2}{\Phi}\exp\left[-\frac{C\Phi^{3/2}}{E_z}\right] , \tag{14}$$

where Φ is the work function of the CNT, and B and C are constants. Computation is performed at every time step, followed by update of the geometry of the CNTs. As a result, the charge distribution among the CNTs also changes and such a change affects Eq. (12). The field emission current (I_{cell}) from the anode surface corresponding to an elemental volume V_{cell} containing an array of CNTs is then obtained as

$$I_{\text{cell}} = A_{\text{cell}}\sum_{j=1}^{N} J_j \ , \tag{15}$$

where A_{cell} is the anode surface area and N is the number of CNTs in the volume element. The total current is obtained by summing the cell-wise current (I_{cell}). This formulation takes into account the effect of CNT tip orientations, and one can perform statistical analysis of the device current for randomly distributed and randomly oriented CNTs.

3. RESULTS AND DISCUSSIONS

In the proposed design of CNT array based field emission, we introduce two additional gates on the edges of the cathode substrate. An array of stacked CNTs is considered on the cathode substrate. The height of the CNTs is such that a symmetric force field is maintained in each pixel with respect to the central axis parallel to z-axis. As a result, it is expected that a maximum current density and well-shaped beam can be produced under

DC voltage across the cathode and anode. In the present design, the anode is assumed to be simply a uniform conducting slab. However, such an anode can be replaced with a porous thin film along with MEMS-based beam control mechanism. Fig. 1 shows the transverse electric field distribution (E_z) in the pixel, which directly influences the field emission from the tip. The side gates are kept at same potential as the cathode substrate. Fig. 2 shows the distribution of electric potential along the CNTs. Clearly, the longer CNTs at the middle is subjected to more than twice the potential at the tip of CNTs at the edge. Fig. 3 shows that the CNT tip at the middle of the array experiences only a slight increase in the electric field and hence an insignificant increase in the electrodynamic pull toward the anode. With this arrangement, it is now possible to tune the spatio-temporal quality of the emitted electron beam. This is analyzed next.

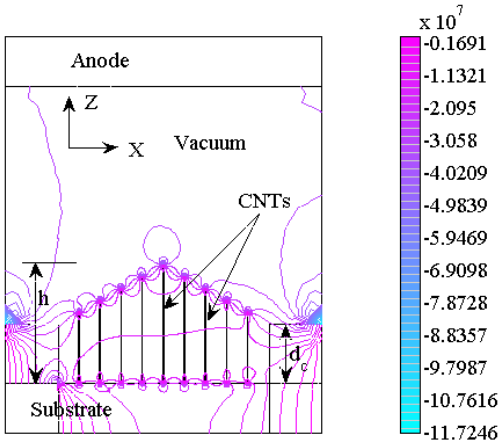

Figure 1. Contour plot showing concentration of electric field E_z surrounding the CNT tips under symmetric lateral force field. $V_0 = 650V$ and the side-wise gates are shorted with the cathode substrate. Electric field contours are shown in V/m unit in the colorbar.

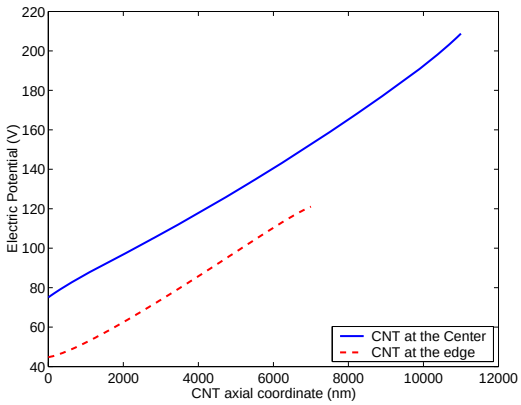

Figure 2. Distribution of electric potential along the CNTs.

In the simulation and analysis, the distance between the cathode substrate and flat anode surface was taken as 34.7μm. The height of the side-wise gates was 6μm, while the spacing between neighboring CNTs in the array was selected as 2μm. A DC bias voltage of 650V is applied across the cathode and anode. We compare the field emission and deformation behaviour of the pointed shape array shown in Fig. 1 with three other array configurations, which are (1) an array with random distribution of height (2) an array with uniform distribution of height and (3) an array with V-shape where the height of the CNTs gradually increases toward the edges. In the case of pointed shape array, the height distribution was varied from 6μm at the edges to 12μm at the centre.

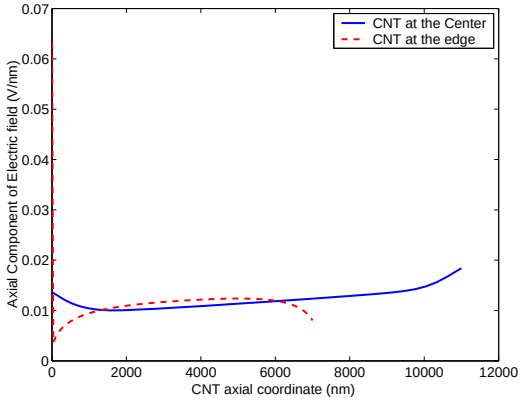

Figure 3. Distribution of transverse electric field E_z along the CNTs.

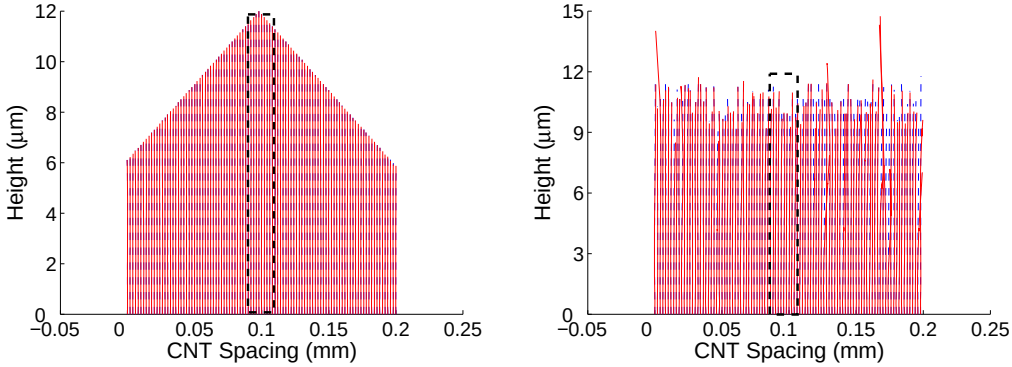

Figure 4. Visualization of initial and deflected shape of an array of 100 CNTs at t= 50s of field emission for (a) pointed (left) and (b) random (right) configurations. The dotted lines indicate initial orientation of the CNTs.

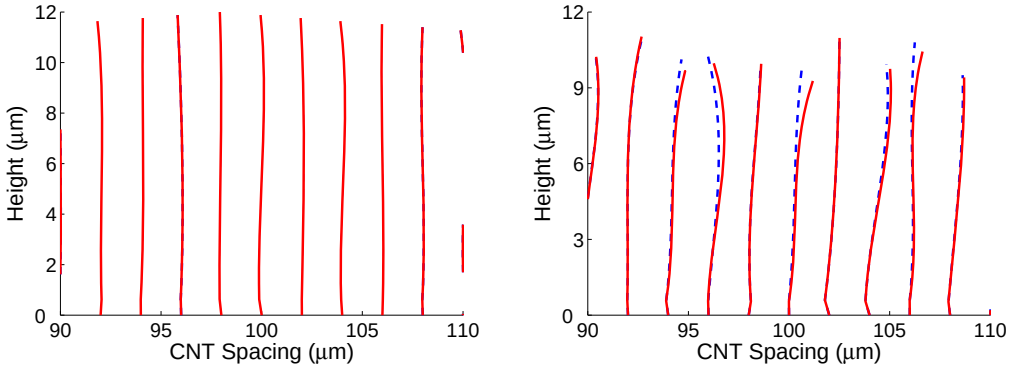

Figure 5. Zoomed middle region of the array showing the deformed CNTs with (a) pointed shape (left) and (b) random height distribution (right). The dotted lines indicate initial orientation of CNTs.

In the case of random height distribution, the height was varied as $h = (h_0 \pm 2\mu m) \mp 2\mu m \times \text{rand}(1)$. Here the function rand denotes random number generator.

Fig. 4(a) shows the stabilized CNTs owing to the electrodynamic interaction due to the pointed shape as compared to the random distribution in Fig. 4(b). Figs. 5(a) and (b) show the zoomed middle region of the two arrays. The tip deflections in the case of random height distribution is as high as 1μm, whereas the deflection in

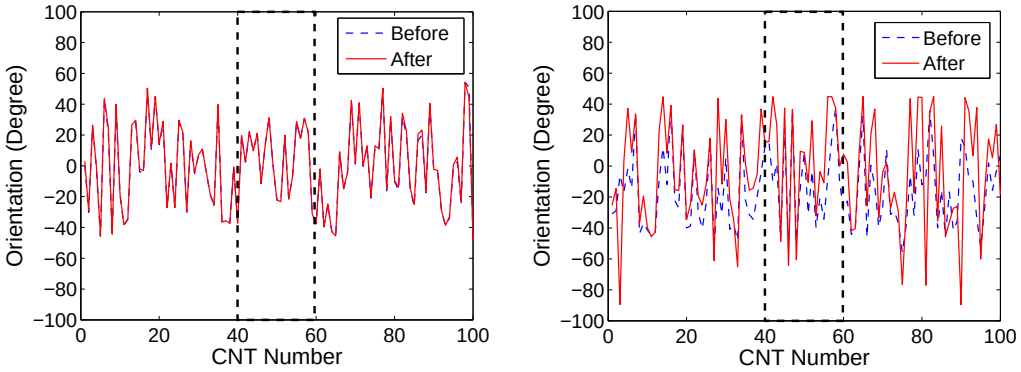

Figure 6. Tip deflections of each CNT in an array of 100 CNTs at t= 50s of field emission for (a) pointed shape (left) and (b) random height distribution (right). The dotted line indicates initial tip orientation angle.

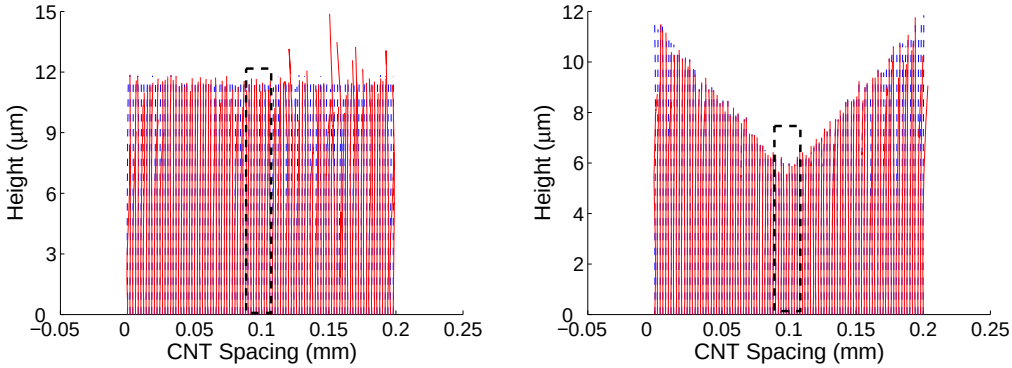

Figure 7. Visualization of initial and deflected shape of an array of 100 CNTs at t= 50s of field emission for (a) uniform height distribution (left) and (b) V-shape (right). The dotted lines indicate initial orientation of the CNTs.

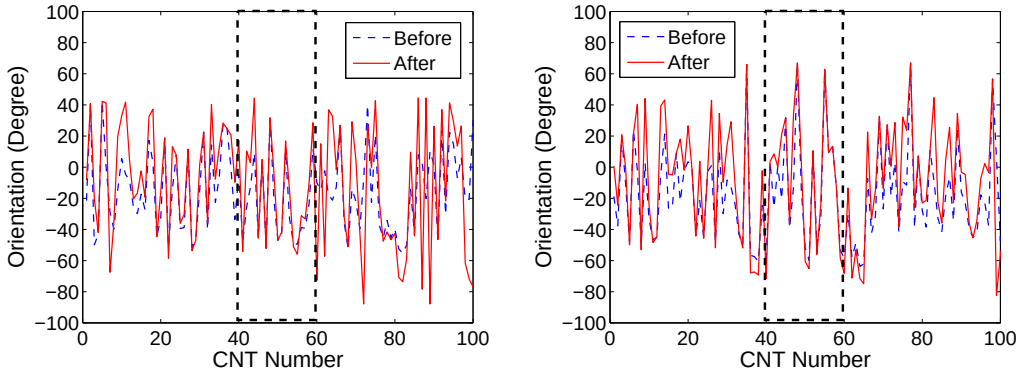

Figure 8. Tip deflections of each CNT in an array of 100 CNTs at t= 50s of field emission for (a) uniform height distribution (left) and (b) V-shape (right). The dotted line indicates initial tip orientation angle.

the case of pointed shape remains within few nanometer which is not visible in Fig. 5(a) and such a phenomenon of improved stability can have many applications. During 50s of field emission simulated in these results, the strong influence of lateral force field can be clearly seen. Such force field produces electrodynamic repulsion such that the resultant force imbalance on the CNTs toward the edges of the array eventually destabilize the orientation of the CNT tips. Since in the pointed shape (see Fig. 4a), this force imbalance is minimized due to gradual

reduction in the CNT heights, a less magnitude of deflections are observed. Also, the lateral electrodynamic force produce instabilities in the randomly distributed array where the electrons are pulled up by the anode and the CNTs tips experiences significant elongation as shown in Fig. 4(b). This is further quantified by the tip angle distribution before and after 50s of field emission as shown in Fig. 6(b) for random height distribution as compared to Fig. 6(a) for the pointed shape. It should be noted that in the simulation, the initial tip deflections are prescribed as random distribution for both the cases. Due to this reason, the tip orientation angles in Fig. 6(a) are also large in the case pointed shape, but these do not change over time. In Figs. 7 and 8, it is shown that uniform height distribution experiences similar instability as in the case of random height distribution, whereas the V-shaped array experiences instabilities near the edges which is a moderate performance among all the four array configurations considered.

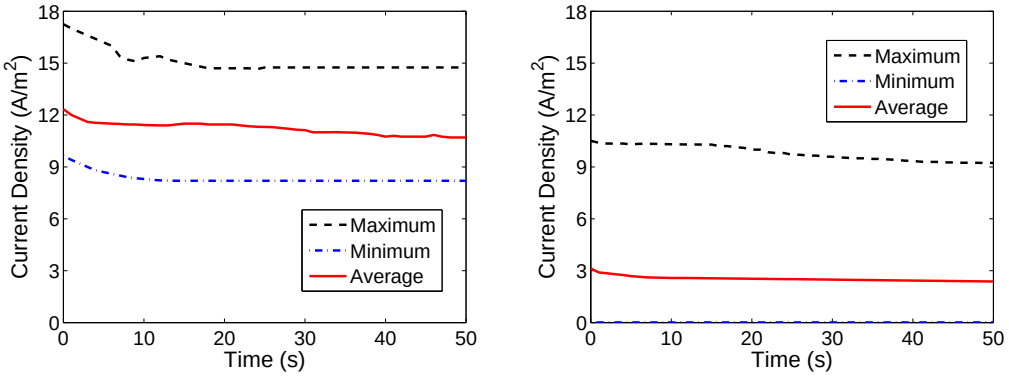

Figure 9. Time histories of field emission current density for array with (a) pointed shape (left) and (b) random height distribution (right).

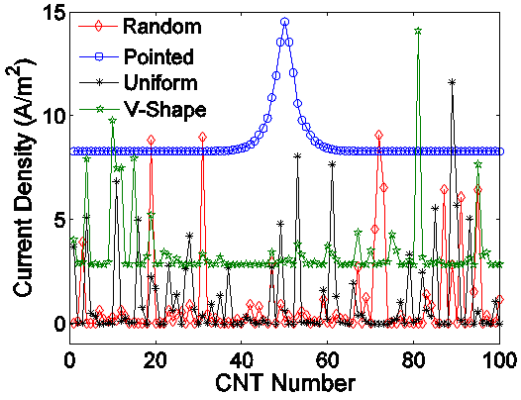

Figure 10. Comparison of current density distribution over CNT arrays of different shapes.

In Figs. 9(a)-(b), we compare the time histories of maximum, minimum and average current density out of different array configurations. It is clearly seen that the pointed shape array shows the best performance with highest average current density and least scatter of emitted electrons over the array. The average current density for the case of pointed shape is almost three times more than the average current density for the case of random height distribution. This is an interesting result, which clearly shows the improvement achieved by using a pointed shape of the array and the side gate. Also, due to lateral foce field induced instabilities in the case of random height distribution, the scatter in the current density distribution in the array is much higher compared to the case of pointed shape. It should also be noted that beside a three fold increase in the magnitude of average current density for the pointed array case in Fig. 9(a), the temporal fluctuation is also insignificant. This indicates an improved field emission with good stability. Fig. 10 shows the spatial distribution of emission

current density in the pointed array as compared to arrays with different shapes. It is clear that the emission is stable and it is focused towards the middle of the array.

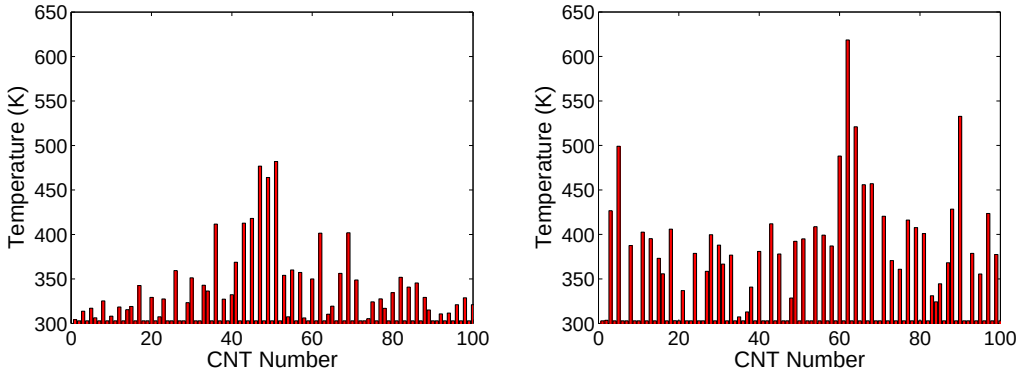

Figure 11. Maximum temperature at the tip of each CNT for an array of 100 CNTs at t = 50s of field emission for (a) pointed shape (left) and (b) random height distribution (right).

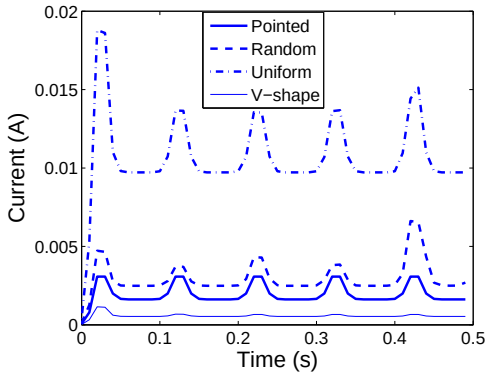

Figure 12. Comparison of field emission current histories for different array types under AC voltage of 650V with frequency of 10Hz.

Temperature at the tip of each CNT over an array of 100 CNTs were computed. Interaction among several quantum states and acoustic-thermal phonon modes take place during the emission of the electronic. As the emitted electrons become ballistic electrons in free space, the corresponding energy released to the CNT cap region produce thermal transients. A mesoscopic model[20] of heat generation and transport in the CNTs from the tip region is employed in the present computation. Fig. 11 shows the temperature at the CNT tips at t=50s for the cases of pointed shape and random height distribution, respectively. Fig. 11(a) shows a temperature rise of up to $\approx$ 480K at the middle of the array. This is less and implies an improved life. Another interesting observation is that the temperature distribution profile shows a more or less gradual decrease toward the edges. On the other hand, as seen in Fig. 11(b), the random height distribution leads to a much stronger electron-phonon interaction as the CNTs undergo large tip rotations. Also, the maximum temperature is nearly 620K and it such a rise is not always at the middle region of the array. Finally, we simulate and compare field emission current histories for different array types under AC voltage of 650V with frequency of 10Hz (see Fig. 12). As evident from Fig. 12, the CNT array with pointed shape gives most stable current output among all the configuraions considered.

4. CONCLUSIONS

In order to obtain stabilized field emission from a stacked CNT array, a new design approach with pointed shape is proposed in this paper. By taking into account various electromechanical forces in the CNTs and transport of conduction electron coupled with electron-phonon induced heat generation from the CNT tips, a mesoscopic modeling technique has been employed in this work. The analysis using a pointed arrangement of the array reveals that the current density distribution is greatly localized at the middle of the array. In addition, the scatter due to electrodynamic force field is minimized and the temperature transients are much smaller compared to those in the arrays with random or uniform height distributions. The V-shaped array shows moderate stability but the the field emission is much smaller compared to the pointed shape array. In pixel form, the pointed shape arrays of CNTs can have useful applications in biomedical x-ray devices and imaging. Based on the proposed idea, a mechanically stable array of CNTs is likely to result in longer life, which is an appealing area of research.

REFERENCES

[1] A. G. Rinzler, J. H. Hafner, P. Nikolaev, L. Lou, S. G. Kim, D. Tomanek, D. Colbert, and R. E. Smalley, *Science* **269**, 1550 (1995).

[2] W. A. de Heer, A. Chatelain, and D. Ugrate, *Science* **270**, 1179 (1995).

[3] L. A. Chernozatonskii, Y. V. Gulyaev, Z. Y. Kosakovskaya, N. I. Sinitsyn, G. V. Torgashov, Y. F. Zakharchenko, E. A. Fedorov, and V. P. Valchuk, *Chem. Phys. Lett.* **233**, 63 (1995).

[4] J. M. Bonard, J. P. Salvetat, T. Stockli, L. Forro, and A. Chatelain, *Appl. Phys. A* **69**, 245 (1999).

[5] Y. Saito, and S. Uemura, *Carbon* **38**, 169 (2000).

[6] H. Sugie, M. Tanemure, V. Filip, K. Iwata, K. Takahashi, and F. Okuyama, *Appl. Phys. Lett.* **78**, 2578 (2001).

[7] P. R. Schwoebel, *Appl. Phys. Lett.* **88**, 113902 (2006).

[8] P. Yaghoobi, and A. Nojeh, *Modern Phys. Lett.* **21**, 1807 (2007).

[9] N. Sinha, D. Roy Mahapatra, J. T. W. Yeow, R. V. N. Melnik, and D. A. Jaffray, *J. comp. Theor. Nanosci.* **4**, 535 (2007).

[10] N. Sinha, D. Roy Mahapatra, Y. Sun, J. T. W. Yeow, R. V. N. Melnik, and D. A. Jaffray, *Nanotechnology* **19**, 025701 (2008).

[11] A. Buldum, and J. P. Liu, *Mol. Sim.* **30**, 199 (2004).

[12] N. Sinha, D. Roy Mahapatra, R. V. N. Melnik, and J. T. W. Yeow, *Lecture Notes in Computer Science* **LNCS 5102**, 197 (2008).

[13] N. Sinha, D. Roy Mahapatra, J. T. W. Yeow, and R. V. N. Melnik, *Proc. IEEE 7th Int. Conf. Nanotech.*, 961 (2007).

[14] M. Wang, Z. H. Li, X. F. Shang, X. Q. Wang, and Y. B. Zu, *J. Appl. Phys.* **98**, 014315 (2005).

[15] G. Chen, D. H. Shin, T. Iwasaki, H. Kawarada, and C. J. Lee, *Nanotechnology* **19**, 415703 (2008).

[16] D. Roy Mahapatra, N. Sinha, S. V. Anand, Vikram N. V., R. V. N. Melnik, and J. T. W. Yeow, *Proc. NSTI-Nanotech 2008* **1**, 55 (2008).

[17] Y. Peng, Y. Hu, and H. Wang, *J. Vac. Sci. Technol.* **25**, 106 (2007).

[18] G. Y. Slepyan, S. A. Maksimenko, A. Lakhtakia, O. Yevtushenko, and A. V. Gusakov, *Phys. Rev. B* **60**, 17136 (1999).

[19] L. Wei, and Y. N. Wang, *Phys. Lett. A* **333**, 303 (2004).

[20] D. Roy Mahapatra, N. Sinha, J. T. W. Yeow, and R. V. N. Melnik, *Appl. Surf. Sci.* **255**, 1959 (2008).

[21] D. Roy Mahapatra, S. Anand, N. Sinha, and R. V. N. Melnik, *Mol. Sim.* **35**, 512 (2009).

[22] A. Svizhenko, M. P. Anantram, and T. R. Govindan, *IEEE Trans. Nanotech.* **4**, 557 (2005).

[23] R. H. Fowler, and L. Nordheim, *Proc. Royal Soc. London A* **119**, 173 (1928).

[24] O. E. Glukhova, A. I. Zhbanov, I. G. Torgashov, N. I. Sinitsyn, G. V. Torgashov, *Appl. Surf. Sci.* **215**, 149 (2003).

[25] A. L. Musatov, N. A. Kiselev, D. N. Zakharov, E. F. Kukovitskii, A. I. Zhbanov, K. R. Izrael'yants, and E. G. Chirkova, *Appl. Surf. Sci.* **183**, 111 (2001).

Contents

Volume 7399: Carbon Nanotubes, Graphene, and Associated Devices II

Editors: Manijeh Razeghi, Didier Pribat, Young-Hee Lee

PROCEEDINGS OF SPIE on CD-ROM

Optics and Photonics 2009: Nanoscience and Engineering

2–6 August 2009
San Diego, California, USA

SPIE Optics+Photonics

SPIE

Volumes 7392–7406

Single-User Edition